Available online at www.sciencedirect.com

ScienceDirect

Genomics 89 (2007) 189–196

GENOMICS

www.elsevier.com/locate/ygeno

# A 1.5-Mb-resolution radiation hybrid map of the cat genome and comparative analysis with the canine and human genomes

William J. Murphy [a,*], Brian Davis [a], Victor A. David [b], Richa Agarwala [c], Alejandro A. Schäffer [d], Alison J. Pearks Wilkerson [a], Beena Neelam [e], Stephen J. O'Brien [b], Marilyn Menotti-Raymond [b,*]

[a] *Department of Veterinary Integrative Biosciences, College of Veterinary Medicine and Biomedical Sciences, Texas A & M University, Mail Stop 4458, College Station, TX 77843, USA*

[b] *Laboratory of Genomic Diversity, Building 560, Room 11-10, National Cancer Institute–Frederick, Frederick, MD 21702, USA*

[c] *Information Engineering Branch, National Center for Biotechnology Information/National Library of Medicine, National Institutes of Health, Department of Health and Human Services, Bethesda, MD 20894, USA*

[d] *Computational Biology Branch, National Center for Biotechnology Information/National Library of Medicine, National Institutes of Health, Department of Health and Human Services, Bethesda, MD 20894, USA*

[e] *Advanced Biomedical Computing Center, National Cancer Institute–Frederick, Frederick, MD 21702, USA*

Received 19 June 2006; accepted 17 August 2006
Available online 25 September 2006

**Abstract**

We report the construction of a 1.5-Mb-resolution radiation hybrid map of the domestic cat genome. This new map includes novel microsatellite loci and markers derived from the 2X genome sequence that target previous gaps in the feline–human comparative map. Ninety-six percent of the 1793 cat markers we mapped have identifiable orthologues in the canine and human genome sequences. The updated autosomal and X-chromosome comparative maps identify 152 cat–human and 134 cat–dog homologous synteny blocks. Comparative analysis shows the marked change in chromosomal evolution in the canid lineage relative to the felid lineage since divergence from their carnivoran ancestor. The canid lineage has a 30-fold difference in the number of interchromosomal rearrangements relative to felids, while the felid lineage has primarily undergone intrachromosomal rearrangements. We have also refined the pseudoautosomal region and boundary in the cat and show that it is markedly longer than those of human or mouse. This improved RH comparative map provides a useful tool to facilitate positional cloning studies in the feline model.


*Keywords:* Domestic cat; Radiation hybrid map; Canine genome; Genome evolution; Synteny; Chromosome rearrangement

Survey-sequenced genomes (i.e., approximately 2X coverage) are useful for providing access to orthology-verified sequences for gene map construction, evolutionary genomic studies, and the annotation of the human genome sequence [1,2]. Nearly 2 dozen mammalian species are in the process of having their genome sequences determined by survey sequencing (http://www.genome.gov/11007951). The recent completion of a 2X domestic cat genome sequence provides a necessary boost for successful application of genome-based scans toward identifying genes of interest in this valuable animal model [3,4]. However, navigating hundreds of thousands of sequence contigs and the remaining traces for a survey-sequenced genome, and confidently establishing their orthology to regions of related mammalian genomes (such as human and dog for cat) using sequence similarity, is a daunting task. This task is less challenging if higher coverage assemblies or high-density comparative maps are available.

Radiation hybrid (RH) maps and linkage maps are important tools for both long-range assembly and quality control of early genome-builds [1,5,6]. We present a new, denser RH map of the domestic cat (*Felis catus*). The marker development phase of this project focused on finding markers in the cat genome sequence traces that were located in holes of the

* Corresponding authors. W.J. Murphy is to be contacted at fax: +1 979 845 9972. M. Menotti-Raymond, fax: +1 301 846 1686.
*E-mail addresses:* wmurphy@cvm.tamu.edu (W.J. Murphy), raymond@mail.ncifcrf.gov (M. Menotti-Raymond).

0888-7543/$ - see front matter © 2006 Elsevier Inc. All rights reserved.
doi:10.1016/j.ygeno.2006.08.007

previous cat–human comparative maps [7–9]. We further combined these new survey sequence-derived markers with a novel collection of feline microsatellite markers. By exploiting the feline genome survey sequence and the close evolutionary relationship with the dog genome, we were able to identify orthologous genome positions in the finished human and canine draft genome sequences for 96% of the markers. We constructed an enhanced comparative map relating the three genomes that provides 86% comparative coverage of the human genome and 85% comparative coverage of the canine genome. With an average spacing of 1 marker every 1.5 Mb in the feline euchromatic sequence, the map provides a solid framework and comparative tool to aid in the identification of genes controlling feline phenotypes and the chromosomal assignment of feline contigs and scaffolds during assembly. Alignment of the feline, canine, and human chromosomes provides insight into the different chromosomal rearrangement characteristics that have occurred in the feline and canine lineages.

## Results

### *Third-generation cat–human and first-generation cat–dog ordered comparative maps*

Combining new high-quality marker genotypes with previous RH data sets [7–9] produced a final set of 1845 markers that were evaluated and used to construct the RH map. After 52 markers were dropped for quality control reasons the final computed RH map includes 1793 markers, with new data from 335 whole genome sequence trace-derived markers, 87 STS markers designed from ESTs and mRNAs, and 269 microsatellite markers. The map contains 1252 maximum likelihood (MLE)-consensus framework markers (see Materials and methods); 1680 markers that have assigned cR positions, including 15 markers that had an identical vector with at least one other marker; and 113 markers that were binned (or placed) relative to the positioned markers. RH map linkage groups were initially established using a two-point lod score threshold of 8.0. For 10 chromosomes the RH linkage groups correspond to separate arms of meta- or submeta-centric chromosomes (A1, A2, B2, B4, C1, C2, D4, E2, E3, and X), and for 8 chromosomes marker density was sufficient to produce single linkage groups for whole chromosomes (A3, B1, B3, D1, D2, D3, F1, and F2). Chromosome E1p formed two RH linkage groups because of the severe changes in retention frequency associated with the RH panel selectable marker (*TK1*) found on this chromosome. These RH groups were merged using evidence from the feline linkage map [8].

The 1793 markers cover all 18 feline autosomes and the X chromosome at an average spacing of 1.5 Mb (Table 1). Excluding the 113 binned markers would produce a marker density of 1 marker/1.6 Mb. Marker density is also fairly uniform between chromosomes (Table 1), with chromosome F1

Table 1
Cat RH map marker summary and comparative map overview

| Feline chromosome | Avg. marker density (Mb) | No. of MLE-consensus framework markers | Total markers on map | RH length ($cR_{5000}$) | Approx physical length[a] (Mb) | cR/Mb | No. of cat-human homologous synteny blocks | Orthologous human chromosomes | No. of cat-dog homologous synteny blocks | Orthologous dog chromosomes |
|---|---|---|---|---|---|---|---|---|---|---|
| A1 | 1.5 | 111 | 168 | 2514.1 | 259 | 9.7 | 15 | 1[b], 5, 13 | 16 | 2, 3, 4, 11, 14[b], 16[b], 22, 25, 34[b] |
| A2 | 1.4 | 107 | 138 | 2143.7 | 189 | 11.3 | 16 | 3, 7, 19 | 9 | 14, 16, 18, 20 |
| A3 | 1.5 | 73 | 99 | 1644.2 | 151 | 10.9 | 13 | 2, 20 | 10 | 10, 17, 23[b], 24 |
| B1 | 1.7 | 93 | 120 | 1926.0 | 208 | 9.3 | 16 | 4, 8 | 15 | 3, 13, 15, 16, 19, 25, 32 |
| B2 | 1.7 | 64 | 90 | 1469.7 | 157 | 9.4 | 4 | 6 | 7 | 1, 12, 35 |
| B3 | 1.5 | 78 | 98 | 1221.5 | 151 | 8.1 | 10 | 14, 15 | 7 | 3, 8, 15[b], 30 |
| B4 | 1.5 | 69 | 100 | 1443.3 | 146 | 9.9 | 3 | 10, 12, 22 | 5 | 2, 10, 15, 27 |
| C1 | 1.6 | 94 | 142 | 2111.0 | 232 | 9.1 | 5 | 1, 2 | 13 | 2, 5, 6, 15, 17, 19, 36, 37 |
| C2 | 1.4 | 81 | 112 | 1533.1 | 157 | 9.8 | 12 | 3, 21 | 10 | 23, 31, 33, 34 |
| D1 | 1.3 | 66 | 100 | 1394.9 | 130 | 10.8 | 6 | 11 | 7 | 5, 18, 21 |
| D2 | 1.4 | 51 | 76 | 1084.7 | 108 | 10.0 | 10 | 1[b], 10 | 6 | 4, 26[b], 28 |
| D3 | 1.4 | 65 | 78 | 1351.2 | 108 | 12.5 | 11 | 12, 18, 22 | 6 | 1, 7, 26 |
| D4 | 1.5 | 55 | 66 | 1184.9 | 100 | 11.9 | 5 | 9 | 4 | 1, 9, 17 |
| E1 | 1.3 | 46 | 77 | 1389.9 | 100 | 13.9 | 6 | 17 | 4 | 5, 9, 18[b] |
| E2 | 1.2 | 36 | 67 | 680.3 | 81 | 8.4 | 2 | 16, 19 | 3 | 1, 2, 5 |
| E3 | 1.4 | 35 | 45 | 697.2 | 62 | 11.2 | 6 | 7, 16 | 4 | 6 |
| F1 | 1.0 | 43 | 76 | 921.8 | 78 | 11.8 | 10 | 1 | 5 | 7, 38 |
| F2 | 1.5 | 33 | 54 | 717.8 | 78 | 9.2 | 1 | 8 | 2 | 13, 29 |
| X | 1.6 | 52 | 87 | 1081.1 | 135 | 8.0 | 1 | X | 1 | X |
| Total | 1.5 | 1252 | 1793 | 26510.3 | 2630 | 10.1 | 152 | | 134 | |

[a] Assumes a 2.7-Mb euchromatic genome and the total cytogenetic fraction estimated for each chromosome in the domestic cat genome [8].
[b] Not detected by Zoo-FISH in previous studies [10–12].

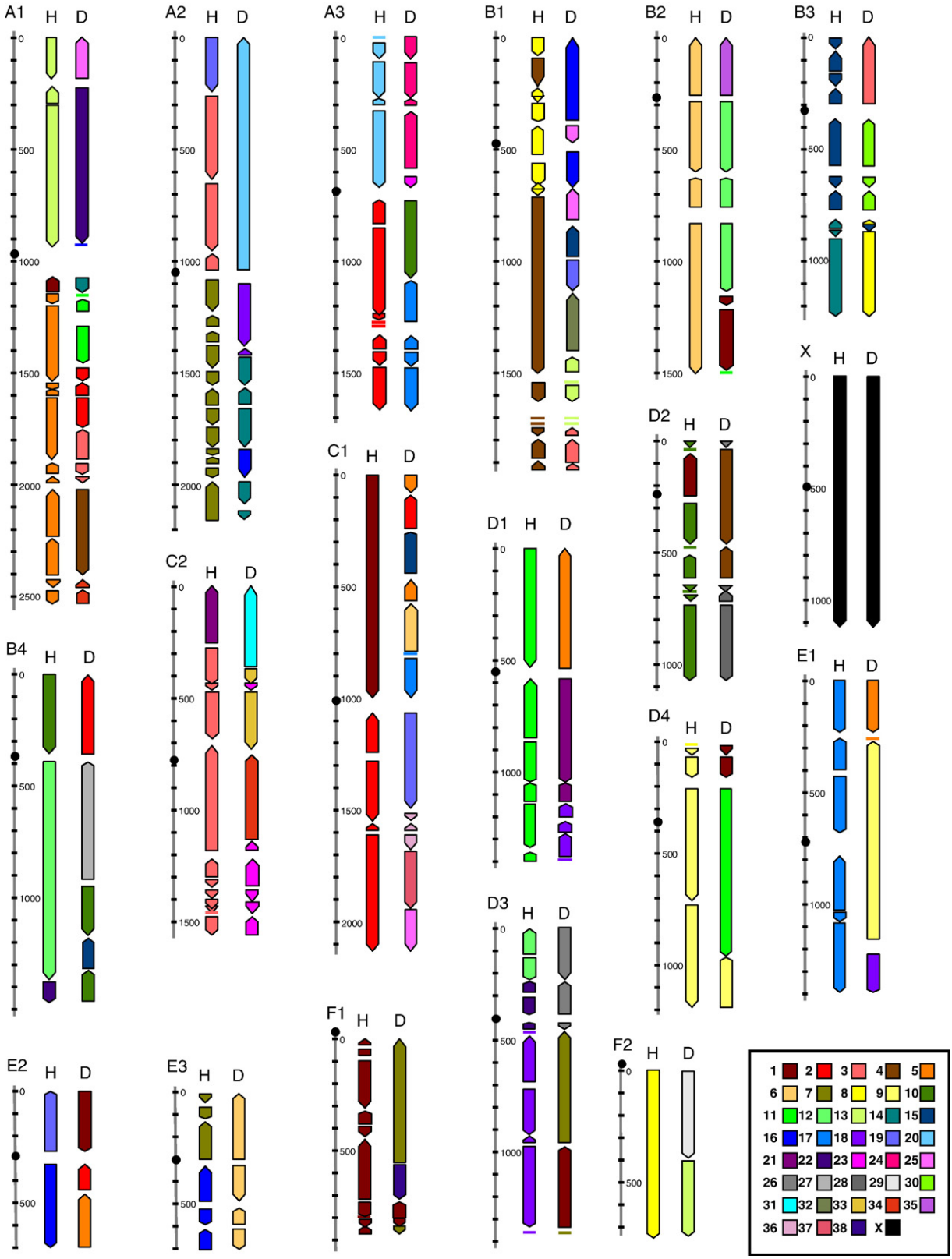


Fig. 1. Feline chromosome maps (labeled at top) and homologous synteny blocks (HSBs) in the human (H) and dog (D) genomes. HSBs are shown to the right of each cat chromosome map (only the map scale is shown). The dark cross-marks on each cat chromosome correspond to 100-cR$_{5000}$ intervals. The inferred centromere positions are shown by dark circles. HSBs are color coded by human or dog chromosome, defined by the key in the bottom right corner.

being the most marker dense at 1 marker/Mb and chromosomes B1 and B2 being the most marker poor at 1 marker/1.7 Mb. Assuming a feline euchromatic genome size of 2.7 Mb based on the assembly of genome survey sequence (Pontius et al., unpublished data), 1 $cR_{5000}$ corresponds to approximately 100 kb, or 10 $cR_{5000}$/Mb (Table 1). The final maps for each chromosome are available in tabular format as supplemental material (Supplemental Table 1), while a graphical display of each cat chromosome and blocks of conserved syntenic order with the human and canine genomes are presented in Fig. 1.

*Comparative synteny analysis*

We identified orthologous positions in the dog and human genomes for 96% of the 1793 markers placed on the final cat RH map (Supplemental Table 1). The resulting comparative maps identify all 32–34 cat–human conserved synteny blocks reported in previous Zoo-FISH studies [10,11], in addition to two smaller blocks of orthology to human chromosome 1 on A1q–cen and D2p not detected by Zoo-FISH (Table 1). We also observed strong concordance with Zoo-FISH maps interrelating the cat and dog genomes, identifying all 68 synteny blocks observed in a previous study comparing cat and dog genomes [12]. The ordering of the canine synteny blocks along the cat chromosomes (Fig. 1) was also consistent between the two approaches, further supporting the long-range ordering of markers on each chromosome.

Taking into account marker order we identified 152 conserved segments (or homologous synteny blocks—HSBs [6,13]) between the cat and the human genomes and 134 between the cat and the dog genomes (Fig. 1). These HSB counts include 13 and 9 comparative singletons in the cat–human and cat–dog comparative maps, respectively; these 22 HSBs are usually singletons in one species and part of a multimarker stretch of conserved gene order in the other species. These singletons likely represent lineage-specific rearrangements. By contrast, we found 18 other "interchromosomal" singletons that appear out of place with respect to all other markers on the same chromosome. Of these, 6 match gene exons that are members of multigene families, suggesting we may have mapped paralogs; the remainder are microsatellites or not gene associated. For the time being, we do not include these singletons in the HSB counts until further mapping validation is performed.

We estimated comparative coverage for all human and dog autosomes and the X chromosomes (Table 2) following previously reported methods [6,14]. Comparative coverage is defined as the sum of the spans of conserved chromosome segments in cat, divided by the size of the human or dog genome after excluding centromere, telomere, and heterochromatic regions [6,14] or regions lacking any cross-species homology in multispecies alignments [13]. Because we were targeting gaps in the cat–human comparative map, we found that our comparative coverage with human was slightly greater than the cat–dog comparative map (86% versus 85%), despite the higher number of breakpoints between cat and human. This may in part be due to the large number of canine-specific intrachromosomal rearrangement breakpoints relative to the more conserved cat chromosomes, for which marker density is low and for which we had no prior comparative mapping information to target. For the cat–human comparison, the mean and median remaining gap sizes are 2.8 and 2.3 Mb, respectively, with 87% of the gaps being less than 5 Mb. Larger gaps remain on several cat chromosomes, notably chromosome D4, where two gaps greater than 9 Mb remain.

Pair-wise counts of cat–human and cat–dog breakpoints reveal slightly more breakpoints between the former (133) compared with the latter (115) (Table 3). However, when adjusted for divergence time, the rate of chromosome breakage is notably higher in the canine lineage (1 breakpoint/million years (Myr)) than in the human lineage (0.70 breakpoints/Myr). Further discrimination between intrachromosomal and interchromosomal breakpoints reveals that within carnivores,

Table 2
Comparative coverage of cat HSBs on dog and human genomes

| Human chromosome | Comp. human length (Mb) | Comp. coverage by cat (%) | Dog chromosome | Comp. canine length (Mb) | Comp. coverage by cat (%) |
|---|---|---|---|---|---|
| 1 | 224 | 89 | 1 | 122 | 80 |
| 2 | 238 | 86 | 2 | 85 | 85 |
| 3 | 195 | 89 | 3 | 92 | 73 |
| 4 | 188 | 85 | 4 | 88 | 97 |
| 5 | 178 | 86 | 5 | 89 | 84 |
| 6 | 167 | 96 | 6 | 76 | 88 |
| 7 | 155 | 76 | 7 | 80 | 94 |
| 8 | 143 | 80 | 8 | 75 | 78 |
| 9 | 114 | 75 | 9 | 51 | 98 |
| 10 | 132 | 79 | 10 | 70 | 92 |
| 11 | 131 | 88 | 11 | 73 | 87 |
| 12 | 131 | 96 | 12 | 72 | 73 |
| 13 | 96 | 90 | 13 | 63 | 72 |
| 14 | 88 | 79 | 14 | 61 | 86 |
| 15 | 82 | 70 | 15 | 64 | 73 |
| 16 | 76 | 91 | 16 | 57 | 89 |
| 17 | 78 | 84 | 17 | 64 | 83 |
| 18 | 75 | 82 | 18 | 63 | 77 |
| 19 | 51 | 92 | 19 | 54 | 89 |
| 20 | 59 | 82 | 20 | 58 | 99 |
| 21 | 33 | 96 | 21 | 50 | 95 |
| 22 | 35 | 74 | 22 | 61 | 96 |
| X | 152 | 99 | 23 | 53 | 76 |
| Total | 2821 | 86 | 24 | 48 | 78 |
| | | | 25 | 51 | 93 |
| | | | 26 | 38 | 68 |
| | | | 27 | 46 | 94 |
| | | | 28 | 39 | 87 |
| | | | 29 | 42 | 86 |
| | | | 30 | 40 | 71 |
| | | | 31 | 38 | 97 |
| | | | 32 | 39 | 94 |
| | | | 33 | 31 | 80 |
| | | | 34 | 42 | 72 |
| | | | 35 | 27 | 95 |
| | | | 36 | 31 | 66 |
| | | | 37 | 31 | 90 |
| | | | 38 | 23 | 65 |
| | | | X | 124 | 98 |
| | | | Total | 2311 | 85 |

Table 3
Chromosomal breakpoint statistics

| Taxon | Interchromosomal breakpoints | Intrachromosomal breakpoints | Total breakpoints | Breakpoints/Myr [a] | Interchromosomal breakpoints/Myr [a] | Intrachromosomal breakpoints/Myr [a] |
|---|---|---|---|---|---|---|
| Cat vs human | 19 | 114 | 133 | 0.70 | 0.10 | 0.60 |
| Cat vs dog | 65 | 50 | 115 | 1.00 | 0.59 | 0.45 |
| Canid-specific [b] | 63 | 8 | 71 | 1.29 | 1.15 | 0.15 |
| Felid-specific [b] | 2 | 42 | 44 | 0.80 | 0.04 | 0.76 |

[a] Assumes a 55-Myr divergence time between cat and dog and a 95-Myr divergence time between cat and human [38].
[b] Determined by comparison to the ancestral carnivore karyotype [16,39].

interchromosomal rearrangements have predominated in the canid lineage (89% of all rearrangements), whereas inversions have been the primary mechanism remodeling felid chromosomes (95% of all rearrangements) since divergence from a common carnivoran ancestor 55 Myr ago (Table 3).

*Refinement of the cat pseudoautosomal boundary*

RH mapping of the most terminal Xp markers produced markedly higher retention frequencies compared to other Xp markers (Fig. 2). Two-point linkage analysis revealed that these markers were strongly linked to existing Y chromosome markers [15] (lod scores ranging between 9 and 13 for markers 39062284, *TBL1X, NLGN4X,* and *SHROOM2*), while weakly linked to X chromosome markers, despite their best BLAST hits and detectable orthology to the X chromosomes of human, mouse, rat, and dog. Inspection of RH vectors revealed that these five markers scored positive (by PCR) for all or nearly all RH panel DNAs containing fragments of the adjacent terminal Xp markers (e.g., *WWC3, 39085624, MID1,* see Supplementary Table 1), but differed from these X chromosome RH vectors only by being positive for clone DNAs that were also positive for feline Y chromosome fragments [15]. Thus, the coamplification of X and Y chromosome fragment RH cell lines is responsible for the anomalously high retention frequencies, and we conclude that these feline markers reside in a pseudoautosomal region (PAR) that is expanded compared to the primate PAR.

## Discussion

We report an updated 1.5-Mb-resolution, RH-based, physical map of the feline genome. This increased marker density resulted in a considerably more detailed cat–human comparative map and a first-generation ordered cat–dog comparative map. Notable improvements include several hundred new markers that more evenly cover previous gaps in the cat–human comparative map, made possible due to access and annotation of domestic cat trace archive sequences. In addition, the close evolutionary relationship between the cat and the dog genomes

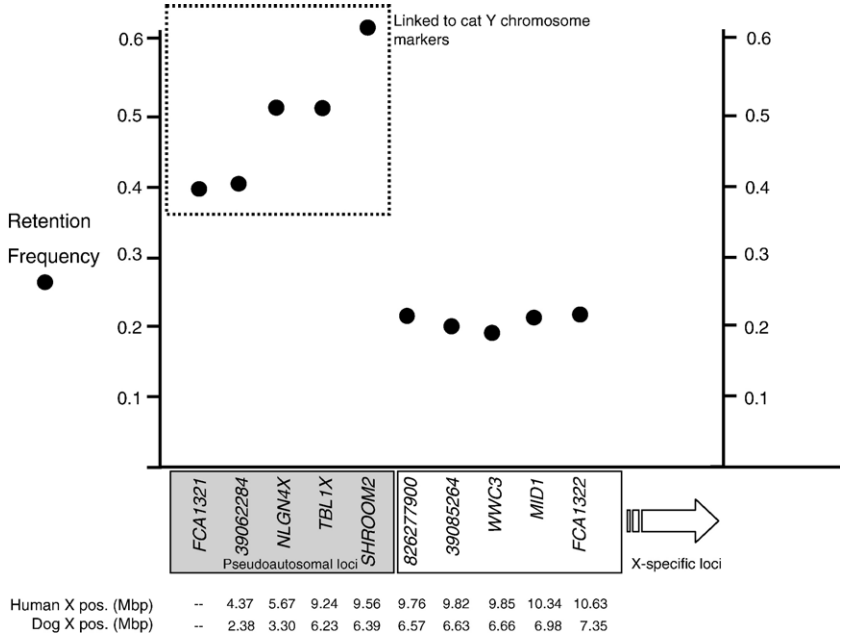


Fig. 2. Putative boundary of the feline pseudoautosomal region as defined by RH STS mapping. The retention frequency is plotted for the most terminal Xp chromosome markers in the cat RH map. The cat markers are listed based on the inferred HSB order with dog and human (Fig. 1). The physical coordinates for each marker (where known) in the dog and human genome sequences are shown below the *x* axis. The pseudoautosomal markers are boxed in gray and are also indicated by their linkage to Y chromosome STS markers (dashed box). X-specific markers have an average retention frequency around 0.20, very similar to the X chromosome-wide average.

allowed for the determination of microsatellite marker orthology between the two carnivoran genomes and the human genome, with a final total of 96% of all mapped feline markers finding positions in both genomes. This is a significant advance over prior versions of the cat–human comparative map in which no feline microsatellite markers were assigned to orthologous regions in the human genome, and only 500–700 gene-based comparative anchors connected the two species' chromosomes [8,9].

With this nearly threefold increase in comparative alignment, we present the first fine-scale syntenic comparison of the cat, dog, and human genomes beyond previous chromosome painting studies [10–12,16]. Classification of breakpoints to different lineages showed a clear increase in the number of breakpoints assigned to the dog lineage relative to cat (Table 3). As was observed by Lindblad-Toh et al. [5], most of the canid-lineage rearrangements are interchromosomal, while most of the rearrangements between the human and the feline genomes are intrachromosomal (inversions). Otherwise our counts and classifications of breakpoints are incomparable to those of Lindblad-Toh et al., in part because they used sequence-based comparison and because some reused breakpoints will be necessarily classified as human-specific rearrangements due to limited taxon sampling.

A striking example of the accelerated rate of evolution in the canid lineage is observed on cat chromosome C1 (Fig. 1, Table 1), on which cat and human share 5 HSBs corresponding to two human chromosomes (1p and 2q), most of the rearrangements being found on C1q (human 2q) due to inversions. By contrast, cat C1 and dog are distinguished by 13 HSBs, most of which are due to translocations involving nine different canine chromosomes. Similar examples of this pattern are seen on two of the other largest cat chromosomes, A1 and B1, on which there are three times the number of cat–dog HSBs compared to cat–human HSBs. Most of this increase is the result of canid-specific interchromosomal rearrangements (Table 1).

After adjusting for evolutionary divergence time, these ordered mapping comparisons confirm the radically rearranged nature of canid chromosome evolution seen by chromosome painting data [12,16]. While felid chromosomes are quite conserved at the syntenic level, even with species from other mammalian orders like human, they have still undergone a fair amount of intrachromosomal rearrangement (0.76/Myr) not appreciated by chromosome painting studies [10,11]. The overall rate of rearrangement within the felid lineage is roughly similar to that between the felid and the human lineage (0.80 versus 0.70). By contrast, canid chromosomes have undergone more than 1.5 times as much total breakage as felid chromosomes, with nearly 30 times as many interchromosomal rearrangements. At present it is not clear what genomic/structural features might explain the different patterns of rearrangement between felids and canids. Full genome comparison of sequence features at chromosome breakpoints in dog and cat genomes remains a fertile area for exploration in the future once better quality genome assemblies become available for both species.

The identification and mapping of PAR markers in the RH panel allowed us to refine the boundary of this region to less than 200 kb between the *SHROOM2* and the *WWC3* genes. Compared to the current human PAR1 boundary near 3 Mb on the X chromosome, the feline (and probably canine) PAR extends as far as 9 Mb on the human X chromosome, though it is still within the limits of an ancient eutherian PAR originally defined by the *AMELX/Y* genes [17]. These findings are consistent with comparative FISH mapping studies of human Xp genes in carnivores and artiodactyls [18] that show the gene content of a formerly larger ancestral PAR1 extended at least as far as the steroid sulfatase (*STS*) gene (~7 Mb on human X), which is still conserved in other eutherian mammals but notably reduced in primates, indicating that the reduction of the ancestral PAR has occurred variably among mammalian lineages [17–19]. Some of the genes in the ancient PAR between 3 and 9 Mb on the human X have evolved Y-specific counterparts, such as *TBL1Y* and *NLGN4Y* [20]. Similarly, the X chromosome counterpart of a recently discovered carnivore-specific Y chromosome gene, *TETY2,* resides just within the *SHROOM2–WWC3* gene interval that currently defines the extent of the felid PAR boundary [15]. This suggests the present felid PAR boundary is a recent carnivore-specific reduction of the formerly larger eutherian PAR [17] that may be shared with the dog. Though not part of the current canine genome annotation [5], further definition of the dog PAR boundary and comparison to cat would be of interest.

Finally, this enhanced mapping resource, coupled with the forthcoming assembly and annotation of the feline genome sequence (Pontius et al., manuscript in preparation), will stimulate and facilitate the identification of feline genes of interest using positional cloning approaches. In the past 3 years 12 feline mutations in nine genes associated with coat color and disease phenotypes have been discovered [21–29]; 6 of these utilized cat genome mapping resources to assess linkage in candidate genes, while the remainder were identified by sequencing candidate genes directly. More recently, the first feline genome scan was used to identify a novel disease gene through positional mapping efforts [4]. With the availability of a detailed comparative map, and integration with developing linkage maps and the 2X sequence, we anticipate that the identification of causative mutations for many feline phenotypes will accelerate, as disease gene mapping has done so recently in the canine model system [30].

## Materials and methods

### *Marker and primer design*

We examined approximately 40,000 random cat 2X traces generated by Agencourt Biosciences and performed BLAST searches with the human and canine genomes. We then chose traces with best reciprocal hits to orthologous regions of both dog and human genomes and used these to design primers for radiation hybrid mapping. Novel microsatellite markers were isolated from a $(dG \cdot dT)_n$ $(dC \cdot dA)_n$ enriched microsatellite library as described [31]. Finally, we designed primers for feline ESTs and mRNAs from GenBank not present on the previous map. All primers were designed with Primer3 [32]. We tested each

primer pair using PCR in cat, hamster, and a 10:1 hamster:cat mixture of DNA, to identify those that produced a single bright band in cat that was absent or of differing mobility compared to hamster.

### *Radiation hybrid genotyping*

RH genotyping for all new gene-based or trace-archive-derived markers was performed using previously described methods [7,8,9]. Genotyping was performed on the 5000-rad feline whole genome radiation hybrid panel [33] and resolved on 2% agarose gels stained with ethidium bromide or scored using a TaqMan-based assay. Markers were dropped before map computation for one of the following reasons: weak amplification, high hamster background amplification, or excessively high retention frequency (>70% and not predicted to reside on the selectable locus chromosome or near a centromere) or excessively low retention frequency compared to other markers on the same chromosome. These new genotypes were merged with vectors from Refs. [7–9] to compile a novel data set. In this process, 24 markers were dropped from eligibility for the new map due to suspect genotypes.

### *Map construction*

Two-point linkage groups were initially computed at a lod score of 8.0, though a small number of markers were included that fell below this threshold due to a number of reasons, such as being close to a centromere, which tends to inflate retention frequencies. These were assigned to chromosomes based on previous physical mapping and FISH and chromosome painting studies [7–11]. Most metacentric and submeta-centric chromosome arms comprised a single linkage group. Gaps generally resulted from high marker retention frequencies near centromeres [7–9]. Three chromosomes comprised multiple linkage groups at LOD=8; these groups were oriented and merged into single groups using best pair-wise lod scores and orientation from linkage maps. Markers within each chromosome arm or linkage group were ordered using a reduction from the problem of RH mapping to the traveling salesman problem (TSP) [34], as implemented in the software rh_tsp_map [35]. The computations to construct the map were done using programs from the software package rh_tsp_map (ftp://ftp.ncbi.nih.gov/pub/agarwala/rhmapping/rh_tsp_map.tar.gz) and using the package CONCORDE (http://www.isye.gatech.edu/~wcook/rh) linked with QSopt (http://www.isye.gatech.edu/~wcook/qsopt) to solve the TSP instances to guaranteed optimality. We followed the multistep procedure used to construct some horse chromosome maps, described in detail in [36]. As in [9,36], we call the first and most reliable map the "MLE-consensus map" because the markers on that map are required to have the same optimal order under three different formulations of the MLE criterion [35]. In addition, we required that in a flips test, the MLE-consensus map be at least 0.5 lod units better than the second best alternative map. One other difference from the procedure in [36] is that for the map herein, 10 markers binned with lod score <0.1 (comparing best placement to second best placement) were placed in a larger interval that combined their best interval with their second best interval.

### *Comparative analysis*

For each domestic cat locus, physical positions for orthologous genes were obtained from the human sequence (build 35). Sequence traces, ESTs, and microsatellites were assigned orthologous positions based upon nucleotide discontiguous MegaBLAST (http://www.ncbi.nlm.nih.gov/blast/) [37] searches to the reference assembly of the dog genome (CanFam1) and the human genome (build 35), using an *E*-value threshold of $e^{-10}$. In cases in which the cat marker found a match only in the dog genome, we identified the corresponding stretch of orthology in the human genome using the dog–human alignment net of the UCSC Genome Browser. Homologous synteny blocks were defined per Ref. [13]. Specifically, we searched for runs of two or more uninterrupted markers on the same chromosome between two species. Inverted segments were defined by runs of three or more markers each separated by 1 Mb. Some out of place markers were expected due to mapping/genotyping errors or limitations of RH mapping resolution. These were assigned to their closest HSB if the intervening markers did not span more than a few megabase pairs. Markers that were binned or placed with a lod score <0.5 were not used in determining marker order, though they could be used to determine the extent of coverage of a HSB.

## Acknowledgments

We thank N. Coomber, S. Corriveau, G. Pei, and T. Raudsepp for technical assistance and/or insightful discussion on these topics. This work was supported by funds from the Winn Feline Foundation and Texas A&M University (W.J.M.). This research was supported in part by the Intramural Research Program of the NIH, NLM (R.A., A.A.S.). This project has been funded in part with federal funds from the National Cancer Institute, National Institutes of Health, under Contract N01-CO-12400 (S.J.O., M.M.-R.). The content of this publication does not necessarily reflect the views or policies of the Department of Health and Human Services, nor does mention of trade names, commercial products, or organizations imply endorsement by the U.S. Government.

## Appendix A. Supplementary data

Supplementary data associated with this article can be found, in the online version, at doi:10.1016/j.ygeno.2006.08.007.

## References

[1] C. Hitte, et al., Facilitating genome navigation: survey sequencing and dense radiation-hybrid gene mapping, Nat. Rev. Genet. 6 (2005) 643–648.
[2] E.H. Margulies, et al., An initial strategy for the systematic identification of functional elements in the human genome by low-redundancy comparative sequencing, Proc. Natl. Acad. Sci. USA 102 (2005) 4795–4800.
[3] S.J. O'Brien, M. Menotti-Raymond, W.J. Murphy, N. Yuhki, The feline genome project, Annu. Rev. Genet. 36 (2002) 657–686.
[4] J.C. Fyfe, et al., An ~140 kb deletion associated with feline spinal muscular atrophy implies an essential *LIX1* function for motor neuron survival, Genome Res. 16 (2006) 1084–1090.
[5] K. Lindblad-Toh, et al., Genome sequence, comparative analysis and haplotype structure of the domestic dog, Nature 438 (2005) 803–819.
[6] A. Everts-van der Wind, et al., A high-resolution whole-genome cattle and human comparative map reveals details of mammalian chromosome evolution, Proc. Natl. Acad. Sci. USA 102 (2005) 18526–18531.
[7] W.J. Murphy, et al., A radiation hybrid map of the cat genome: implications for comparative mapping, Genome Res. 10 (2000) 691–702.
[8] M. Menotti-Raymond, et al., Second-generation integrated genetic linkage/radiation hybrid maps of the domestic cat (*Felis catus*), J. Hered. 94 (2003) 95–104.
[9] M. Menotti-Raymond, et al., Radiation hybrid mapping of 304 novel microsatellites in the domestic cat genome, Cytogenet. Genome Res. 102 (2003) 272–276.
[10] G. Rettenberger, et al., ZOO-FISH analysis: cat and human karyotypes closely resemble the putative ancestral mammalian karyotype, Chromosome Res. 3 (1995) 479–486.
[11] J. Wienberg, et al., Conservation of human versus feline genome organization revealed by reciprocal chromosome painting, Cytogenet. Cell Genet. 77 (1997) 211–217.
[12] F. Yang, et al., Reciprocal chromosome painting illuminates the history of genome evolution of the domestic cat, dog and human, Chromosome Res. 8 (2000) 393–404.
[13] W.J. Murphy, et al., Dynamics of mammalian chromosome evolution inferred from multispecies comparative maps, Science 309 (2005) 613–617.
[14] S.N. Meyers, et al., Piggy-BACing the human genome. II. A high-

resolution, physically anchored, comparative map of the porcine autosomes, Genomics 86 (2005) 739–752.
[15] W.J. Murphy, et al., Novel gene acquisition on carnivore Y chromosomes, PLoS Genet. 2 (2006) 353–363.
[16] W.G. Nash, J.C. Menninger, J. Wienberg, H.M. Padilla-Nash, S.J. O'Brien, The pattern of phylogenomic evolution of the Canidae, Cytogenet. Cell Genet. 95 (2001) 210–224.
[17] M. Iwase, et al., The amelogenin loci span an ancient pseudoautosomal boundary in diverse mammalian species, Proc. Natl. Acad. Sci. USA 100 (2003) 5258–5263.
[18] R. Toder, et al., Genes located in and near the human pseudoautosomal region are located in the X and Y pairing region in dog and sheep, Chromosome Res. 5 (1997) 301–306.
[19] S.H. Park, et al., Rapid divergency of rodent CD99 orthologs: implications for the evolution of the pseudoautosomal region, Gene 353 (2005) 177–188.
[20] M.T. Ross, et al., The DNA sequence of the human X chromosome, Nature 434 (2005) 325–337.
[21] E. Eizirik, et al., Molecular genetics and evolution of melanism in the cat family, Curr. Biol. 13 (2003) 448–453.
[22] K.L. Somers, et al., Mutation analysis of feline Niemann and Pick C1 disease, Mol. Genet. Metab. 79 (2003) 99–103.
[23] L.A. Lyons, et al., Feline polycystic kidney disease mutation identified in PKD1, J. Am. Soc. Nephrol. 15 (2004) 2548–2555.
[24] L.A. Lyons, D.L. Imes, H.C. Rah, R.A. Grahn, Tyrosinase mutations associated with Siamese and Burmese patterns in the domestic cat (*Felis catus*), Anim. Genet. 36 (2005) 119–126.
[25] A. Schmidt-Küntzel, E. Eizirik, S.J. O'Brien, M. Menotti-Raymond, Tyrosinase and tyrosinase related protein 1 alleles specify domestic cat coat color phenotypes of the albino and brown loci, J. Hered. 96 (2005) 289–301.
[26] L.A. Lyons, I.T. Foe, H.C. Rah, R.A. Grahn, Chocolate coated cats: TYRP1 mutations for brown color in domestic cats, Mamm. Genome. 16 (2005) 356–366.
[27] M. Goree, J.L. Catalfamo, S. Aber, M.K. Boudreaux, Characterization of the mutations causing hemophilia B in 2 domestic cats, J. Vet. Intern. Med. 19 (2005) 200–204.
[28] K.M. Meurs, et al., A cardiac myosin binding protein C mutation in the Maine coon cat with familial hypertrophic cardiomyopathy, Hum. Mol. Genet. 14 (2005) 3587–3593.
[29] D.L. Imes, L.A. Geary, R.A. Grahn, L.A. Lyons, Albinism in the domestic cat (Felis catus) is associated with a tyrosinase (TYR) mutation, Anim. Genet. 37 (2006) 175–178.
[30] H.G. Parker, E.A. Ostrander, Canine genomics and genetics: running with the pack, PLoS Genet. 1 (2005) 507–513.
[31] R. Sarno, V.A. David, W.L. Franklin, S.J. O'Brien, W.E. Johnson, Development of microsatellite markers in the guanaco, *Lama guanicoe:* utility for South American camelids, Mol. Ecol. 9 (2000) 1922–1924.
[32] S. Rozen, H. Skaletsky, Primer3 on the WWW for general users and for biologist programmers, in: S. Krawetz, S. Misener (Eds.), Bioinformatics Methods and Protocols: Methods in Molecular Biology, Humana Press, Totowa, NJ, 2000, p. 365.
[33] W.J. Murphy, M. Menotti-Raymond, L.A. Lyons, M.A. Thompson, S.J. O'Brien, Development of a feline whole genome radiation hybrid panel and comparative mapping of human chromosome 12 and 22 loci, Genomics 57 (1999) 1–8.
[34] D. Applegate, R. Bixby, V. Chvátal, W. Cook, On the solution of traveling salesman problems, Documenta Mathematica, extra volume, III, International Congress of Mathematics, 1998, pp. 645–656.
[35] R. Agarwala, D.L. Applegate, D. Maglott, G.D. Schuler, A.A. Schäffer, A fast and scalable radiation hybrid map construction and integration strategy, Genome Res. 10 (2000) 350–364.
[36] C. Brinkmeyer-Langford, et al., A high-resolution physical map of equine homologues of HSA19 shows divergent evolution compared to other mammals, Mamm. Genome 16 (2005) 631–649.
[37] Z. Zhang, S. Schwartz, L. Wagner, W. Miller, A greedy algorithm for aligning DNA sequences, J. Comp. Biol. 7 (2000) 203–214.
[38] M.S. Springer, W.J. Murphy, E. Eizirik, S.J. O'Brien, Placental mammal diversification and the Cretaceous and Tertiary boundary, Proc. Natl. Acad. Sci. USA 100 (2003) 1056–1061.
[39] W.J. Murphy, R. Stanyon, S.J. O'Brien, Evolution of mammalian genome organization inferred through comparative gene mapping, Genome Biol. 2 (2001) 0005.1–0005.8.